IEEE Access
Multidisciplinary ⋮ Rapid Review ⋮ Open Access Journal

Received February 11, 2020, accepted February 29, 2020, date of publication March 6, 2020, date of current version April 9, 2020.

Digital Object Identifier 10.1109/ACCESS.2020.2979050

Peak Shaving Model for Coordinated Hydro-Wind-Solar System Serving Local and Multiple Receiving Power Grids via HVDC Transmission Lines

BENXI LIU[1,2], JAY R. LUND[3], SHENGLI LIAO[1,2], XIAOYU JIN[1,2], LINGJUN LIU[1,2], AND CHUNTIAN CHENG[1,2]

[1]Institute of Hydropower and Hydroinformatics, Dalian University of Technology, Dalian 116024, China
[2]Key Laboratory of Ocean Energy Utilization and Energy Conservation, Ministry of Education, Dalian University of Technology, Dalian 116024, China
[3]Department of Civil and Environmental Engineering, University of California at Davis, Davis, CA 95616, USA

Corresponding author: Shengli Liao (shengliliao@dlut.edu.cn)

This work was supported in part by the National Natural Science Foundation of China under Grant 51709035 and Grant 51979023, in part by the China Scholarship Council under Grant 201806065023, and in part by the Fundamental Research Funds for the Central Universities under Grant DUT19TD32.

ABSTRACT To meet the rapid growth of electricity demand and reduce carbon intensity, China is developing renewable energies rapidly including hydropower, wind and solar power. Due to the geographical mismatch of energy sources and demands in China, many long-distance and large-scale UHVDC and HVDC transmission projects have been built to transmit electric power from the western renewable bases to eastern coastal load centers. Some provincial power sources serve both local demands and deliver power to multiple regional power grids via HVDC transmission lines. As large capacity HVDC power transmission projects have great impacts on receiving-end power grids. Thus, the local exporting power grid should consider both local demands and energy importing area demands. A mixed-integer linear programming day-ahead peak shaving model to minimize the peak-valley difference in residual load after renewable generation of multiple power grids is developed. The model uses chance constraints to compensate for forecast errors of wind and solar power with hydropower, and introduces maximum daily power regulation times and stair-like power curve constraints of HVDC tie lines to avoid frequent HVDC power change and ensure power grid safety. The case studies in Yunnan province, which has large scale hydro, wind and solar power sources and delivers power to multiple regional power grids via HVDC transmission lines, shows the proposed model can shave peaks from multiple power grids effectively, hydropower can compensate for wind and solar forecast error and obtain satisfying results for multiple power grids, and that HVDC constraints can avoid their frequent power change and ensure the power grid safety.

INDEX TERMS Hydro-wind-solar, peak shaving operation, mixed-integer linear programming, HVDC.

NOMENCLATURE

A. ACRONYMS

HVAC	High-voltage alternating current
HVDC	High-voltage direct current
UHVDC	Ultra-high-voltage direct current
CHS	Cascaded hydropower system
LCCHS	Lancang river cascaded hydropower system
JSCHS	Jinsha river cascaded hydropower system
YNPG	Yunnan power grid
GDPG	Guangdong power grid
GXPG	Guangxi power grid

B. SETS AND INDICES

G, g	Number of grids and index of power grid.
T, t	Set and index of time periods
M, m	Set and index of hydropower plants

The associate editor coordinating the review of this manuscript and approving it for publication was Siqi Bu.

K_m, k	Set and index of discrete discharge-output curves of hydropower plant
L, l	Set and index of piecewise discharge-output performance curve
R, r	Set and index of HVDC transmission line
Ω_g	HVDC transmission line sets serving for power grid g
Ω_m	upstream hydropower plant set of plant m

C. PARAMETERS AND VARIABLE

n_t	Number of samples
$x_{t,i}$	Value of sample i
$x^W_{t,i}$	Forecast error sample i of wind power
$x^S_{t,i}$	Forecast error sample i of solar power
$P^{W,a}_{t,i}$	Actual output sample i of wind power
$P^{W,f}_{t,i}$	Forecast output sample i of wind power
$P^{S,a}_{t,i}$	Actual output sample i of solar power
$P^{S,f}_{t,i}$	Forecast output sample i of solar power
$L_{g,t}$	Primal load of power grid g at period t
$P_{g,t}$	Receiving power of grid g at period t
$D_{g,t}$	Residual load of power grid g at period t
δ_g	load reserve rate of grid g
$P^L_{l,t}$	transmission power of line l at period t
$\underline{P}^L_l$, $\bar{P}^L_l$	lower and upper transmission capacity of line l
ω_g	Weight of power grid g in objective function
$P_{r,t}$	Power of HVDC transmission line r at period t
P_t	Total output of hybrid hydro-wind-solar system at period t
$P^{H,max}_{m,t}$	Available maximum output of hydropower plant m at period t
$P^{H,min}_{m,t}$	Available minimum output of hydropower plant m at period t
$P^H_{m,t}$	Output of hydropower m at period t
$\Delta\bar{P}^H_m$	max power ramping capacity of plant m
$P^{W,f}_t$	Forecast output of aggregated wind power at period t
$P^{W,a}_t$	Actual output of aggregated wind power at period t
$P^{S,f}_t$	Forecast output of aggregated solar power at period t
$P^{S,a}_t$	Actual output of aggregated solar power at period t
A_g	Upper boundary of residual load of power grid g
B_g	Lower boundary of residual load of power grid g
$\underline{P}_r$, $\overline{P}_r$	Lower and upper power limits of HVDC line r
$\Delta P^+_{r,t}$, $\Delta P^-_{r,t}$	Positive and negative power change of HVDC line r at period t
$\Delta\bar{P}^+_r$, $\Delta\bar{P}^-_r$	Upper and lower change limit of HVDC line r at period t.
$b^+_{r,t}$, $b^-_{r,t}$	Binary variables to mark if power change of HVDC line r is positive or negative at period t.
T^M_r	Minimum continue periods that power of HVDC transmission line r should keep static or keep change in single direction
$u^+_{r,t}$, $u^-_{r,t}$	Binary variable to mark if the power is change positive of negative during the stair periods
C_r	Allowable daily power change times of HVDC line r
$\underline{E}_g$, $\overline{E}_g$	Lower and upper limits of daily electricity delivered to power grid g
α	Positive compensate confidence level
β	Negative compensate confidence level
$S_{m,t}$	Storage of reservoir m at period t.
$\tau_{j,m}$	water transportation time periods from hydropower plant j to m
$Q^{in}_{m,t}$	natural incremental inflow of plant m at period t
$Q^s_{m,t}$	spill of plant m at period t
$Q^{tur}_{m,t}$	turbine discharge of plant m at period t
$Q^{out}_{m,t}$	total discharge of plant m at period t
$\underline{S}_{m,t}$, $\bar{S}_{m,t}$	Lower and upper storage limit of reservoir m at period t
$\underline{Q}^{out}_{m,t}$, $\bar{Q}^{out}_{m,t}$	Lower and upper discharge limits of reservoir m at period t
$\underline{Q}^{tur}_{m,t}$, $\bar{Q}^{tur}_{m,t}$	Lower and upper turbine discharge limits of reservoir m at period t
$S_{m,beg}$	Initial storage of reservoir m
$S_{m,end}$	Expected final storage of reservoir m
$Z^{up}_{m,t}$	Forebay water level of reservoir m at period t
$Z^{down}_{m,t}$	Tail water level of reservoir m at period t
$H_{m,t}$	Net head of reservoir m at period t
$H^{loss}_{m,t}$	Head loss of reservoir m at period t
$a_{l,k}$	Slope of piecewise linearization hydropower performance curve segment l
$q_{l,k}$	Turbine flow of piecewise linearization segment l
$\bar{q}_{l,k}$	Up limit of piecewise linearization turbine flow of l
$v_{m,k}$	Binary variable indicate if the current storage is between $S_{m,k}$ and $S_{m,k+1}$

D. FUNCTIONS

$\hat{f}_t(\cdot)$	Estimated probability density function
$\hat{f}^W_t(\cdot)$	Estimated probability density function of wind power

$\hat{f}_t^S(\cdot)$	Estimated probability density function of solar power
$K(\cdot)$	Gaussian kernel function
$\Pr\{\cdot\}$	Probability function of chance constraint
$F_t^{W-1}(\cdot)$	Inverse function of wind power forecast error cumulative probability function
$F_t^{S-1}(\cdot)$	Inverse function of solar power forecast error cumulative probability function
$f_m^{gen}(\cdot)$	Hydropower plant generation performance function
$f_m^{ZV}(\cdot)$	Hydropower forebay water level-storage function
$f_m^{ZQ}(\cdot)$	Hydropower tail water level - discharge function
$f_m^{loss}(\cdot)$	Hydropower head loss – turbine discharge function

I. INTRODUCTION

China has seen fast economic development and rapid electricity demand growth in recent years [1]. However, electricity generation is mainly from coal-fired thermal power, and China seeks to reduce carbon intensity by 60%-65% in 2030 compared to 2005 [2]. China is developing large scale clean energy sources and is the biggest contributor of new clean supplies in recent years [3]. By the end of 2018, installed capacity of hydropower, wind and PV has reached 362 GW, 184 GW and 175 GW [4], accounting for about 27%, 33% and 35% of the global capacity respectively [5]. However, most cleaner energy sources are in western China while 75% percent of energy demand is along the east coastal provinces [6]. The huge geographic mismatch between China's clean energy bases (in the west) and the load centers (in the east and southeast) requires a massive transmission network to move electricity from west to east across long distances [7]–[9]. For long distance transmission, high voltage alternating current (HVAC) system may be tricky for sending and receiving power [10]. High-voltage direct current (HVDC) power transmission systems do not require synchronizing power cycles across host and client regions, can stabilize the power system with rapid changes with minimal impact on power system [11]. Moreover, HVDC systems are environmentally superior and have lower investment cost for bulk and long-distance power transmission compared to HVAC, enhance power system controllability and reduce carbon emissions and power loss [12]. Thus, China has built extensive HVDC and ultra-high-voltage direct current (UHVDC) transmission projects to facilitate bulk power transfers [13], [14]. Currently, China has commissioned fourteen UHVDC transmission projects, include thirteen ±800kV lines, and the left one is the world's highest voltage level, longest distance and largest capacity Changji - Guquan transmission project, with voltage of ±1100 kV over 3324 km with a capacity of 12 GW. HVDC and UHVDC systems have become the backbone transmission network for China to deliver bulk electric power from west to east.

Renewable energies like wind and solar power are growing rapidly. But they are characterized by intermittency and uncertainty, making it sometimes difficult for the power grid to accept large scale uncertain wind and solar power directly. So, integrating conventional power sources like thermal and hydropower with renewable energies is a modern reality. In this integration, hydropower has the advantages of fast response and large quantity energy storage [15]. Some models and methods have been introduced to coordinate operate renewable energies with traditional thermal/hydro power plants [16]–[18]. Many studies have been published on coordinate operation or complement operation of hydro-wind [19], hydro-wind-solar [20]–[22] and hydro-thermal-wind-solar power sources [23].

These studies mainly focused on compensating wind and solar power with thermal/hydro power in the same regional power grid. Since HVDC transmission lines have become the backbone of long-distance bulk power transmission, there have been some studies on bundle transmission of renewable energies with traditional hydro/thermal powers via HVDC transmission lines [24]–[26]. Su *et al.* [27] proposed a day-ahead scheduling model for wind power and pumped-storage hydropower (PSH) integrated transmission via ultra-high voltage transmission lines, this model uses PSH to alleviate the uncertainty of wind power. Xie *et al.* [28] introduced a planning model to optimize bundled wind-thermal power system via HVDC transmission lines, considering the compensating capacity of thermal power and the cost of HVDC transmission lines. Xu *et al.* [29] proposed a multi-objective optimal scheduling model for bundled wind, solar and pumped storage plants transmit via HVDC transmission lines, with the objective of maximize renewable energy consumption and minimize power fluctuation. Some other studies focus on how to allocate the power in the receiving power grid. Shen *et al.* [30] built an integrated framework for coordinating HVDC import power with regional power sources to alleviate peak shaving pressure, assuming the energy transmitted by HVDC is given and does not consider the host power grid's power sources. Feng *et al.* [31] developed a model to allocate long distance power to minimize the weighted peak-valley difference in the receiving regional power grid. These studies mainly focus on scheduling on power generation side or allocating HVDC receiving power properly. Few studies examine both sending and receiving power grids simultaneously and the operation constraints of HVDC lines at the same time. In China, some huge cascaded hydropower system (CHS) deliver power to both the local power grid and other regions via HVDC systems, even to multiple regional power grids, and compensate wind and solar power uncertainty and variability as well. Scheduling in a hydro-wind-solar system needs to consider requirements of both sending and receiving power grids.

Peak operation is essential for day-ahead scheduling of power grids. Many studies have been published on hydropower peak shaving or hydro-wind-solar system peak operation. For example, Shen *et al.* [32] develops a load

subsection optimization model to allocate hydrothermal generation for peak operation of multiple provincial power grids. Feng *et al.* [33] provides a parallel progressive optimality algorithm for day-ahead hydropower peak shaving operation. Wu *et al.* [34] devotes a multi-objective hydropower scheduling model for peak shaving of multiple power girds. Wang *et al.* [35] develops a short-term hybrid hydro-thermal-wind coordinate operation model considering hydropower-wind compensation. Notton *et al.* [36] gives a simulation tool for peak shaving of an island with hybrid solar, wind and pumped storage hydropower plant. Cheng *et al.* [37] proposes a hybrid algorithm to optimize pumped storage hydropower plant serving peak shaving operation for multiple power grids.

With growing power demand, the peak-valley difference is expanding rapidly, posing a challenge for power dispatching. Due to continuous growth of load and its peak-valley difference, with large-scale integration of external power does not conform to the receiving ends' load curve greatly challenge peak shaving for receiving power grids. Coordinating the operation of hybrid power sources and HVDC transmission lines to shave peak loads of both local and multiple receiving-end regional power grids is a feasible solution. However, frequent adjustment of HVDC power may require complex adjustments of both exporting and importing grids, which may induce HVDC system failures and large-scale power system failure. So, dispatching department usually considers limited power adjustment times in actual HVDC system scheduling. This study presents a model for day-ahead scheduling of hybrid hydro-wind-solar power system which serving power for the local power grid and multiple receiving power grids via HVDC transmission lines. The objective of this model is to smooth residual loads across multiple power grids. This model aggregates all wind power plants into a virtual wind power plant and all solar power plants into a virtual solar power plant, uses hydropower to compensate for forecast errors of wind and solar power within chance constraints and considers constraints on daily regulation times and other operation constraints of HVDC transmission lines. There are differences between previous studies and this one. This paper makes three contributions:

1) A day-ahead hybrid hydro-wind-solar coordinated model considering peak shaving of both the local power grid and multiple HVDC transmission receiving power grids is proposed.

2) This model considers uncertainty of wind and solar power as chance constraints, considers daily power regulation time constraints and stair-like power curve constraint of HVDC transmission lines.

3) This model is cast as a mixed-integer linear programming (MILP) problem and case studies verified the effectiveness of the proposed model.

The rest of this paper is organized as follows. Section 2 introduces the study area. Section 3 describes the model formulation, constraints and recasts the model to a MILP solvable problem. Case studies and discussion are presented in section 4. Finally, Section 5 gives conclusions and possible further studies.

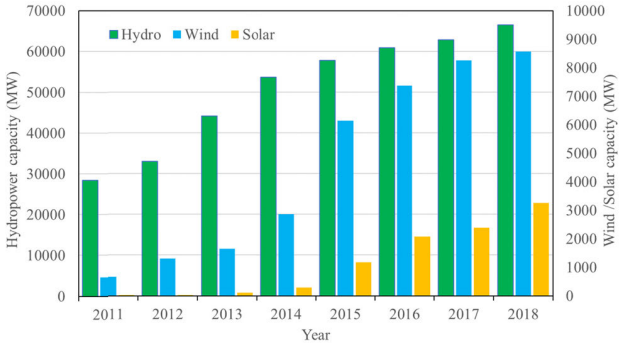

FIGURE 1. The evolution of installed capacity of hydro, wind and solar power in Yunnan. Data source:[4], [40].

II. STUDY AREA: YUNNAN, POWERHOUSE OF SOUTH CORRIDOR OF WEST TO EAST POWER TRANSMISSION

Yunnan province is in southwest China. With several large rivers and large elevation differences from northwest to southeast, it has immense hydropower resources [1]. With implementation of the ''Western Development'' strategy and ''West to East Power Transmission'' (WEPT), Yunnan's hydropower developed fast, its installed capacity surged from 28,420 MW in 2011 to 66,488 MW by 2018, concentrated in Lancang and Jinsha river basins. Yunnan also has great wind and solar power resources [38], these two kinds of renewable power sources also have developed rapidly in recent years. Fig. 1 shows that the installed capacity of wind and solar power in Yunnan has surged from 670 MW and 20 MW in 2011 to 8,573 MW and 3,262 MW by 2018, respectively. As the powerhouse of south corridor of WEPT (in Fig. 2), Yunnan delivers electricity to Guangdong and Guangxi via HVDC lines, with an important role for reducing carbon density. In 2018, the transmitted electricity from Yunnan to Guangdong and Guangxi was 124.6 trillion Watt-hour (TWh) and 13.4 TWh, about 19.7% and 7.9% of these provinces' annual electricity consumption, and about 49.2% of Yunnan's annual electricity generation, is an import supplier for both Guangdong and Guangxi [39]. With continuing development of hydropower and other renewable sources and corresponding HVDC transmission lines, Yunnan will be a more essential electric power supplier for Guangdong and Guangxi.

With fast development of wind and solar power, their characteristics of intermittency and uncertainty has impacted power dispatching, especially for peak shaving. Furthermore, larger and larger peak-valley difference and limited flexible power sources increase peak shaving operation problems. As Yunnan not only supplies electric power for itself, but also exports to Guangdong and Guangxi, it needs to consider peak shaving over multiple provincial power grids.

Since the Lancang cascaded hydropower system (LCCHS) and Jinsha cascaded hydropower system (JSCHS) dominate

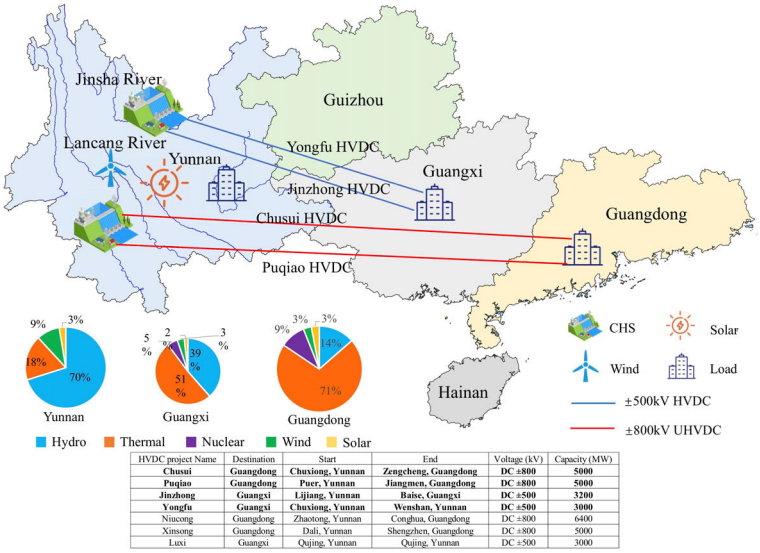

HVDC project Name	Destination	Start	End	Voltage (kV)	Capacity (MW)
Chusui	**Guangdong**	**Chuxiong, Yunnan**	**Zengcheng, Guangdong**	**DC ±800**	**5000**
Puqiao	**Guangdong**	**Puer, Yunnan**	**Jiangmen, Guangdong**	**DC ±800**	**5000**
Jinzhong	**Guangxi**	**Lijiang, Yunnan**	**Baise, Guangxi**	**DC ±500**	**3200**
Yongfu	**Guangxi**	**Chuxiong, Yunnan**	**Wenshan, Yunnan**	**DC ±500**	**3000**
Niucong	Guangdong	Zhaotong, Yunnan	Conghua, Guangdong	DC ±800	6400
Xinsong	Guangdong	Dali, Yunnan	Shengzhen, Guangdong	DC ±800	5000
Luxi	Guangxi	Qujing, Yunnan	Qujing, Yunnan	DC ±500	3000

FIGURE 2. Sketch map of China Southern power grid and electricity transmission lines from Yunnan to Guangdong and Guangxi. Note: This paper concentrates on bolded Chusui, Puqiao, Jinzhong, Yongfu HVDC transmission lines which mainly transmit hydropower from lower Lancang and middle Jinsha cascaded hydropower systems to Guangdong and Guangxi.

TABLE 1. Basic information of the studied cascaded hydropower systems.

CHS	Plant	Installed Capacity (MW)	Regulating Capability	Storage ($10^8 m^3$)
Lower Lancang cascaded hydropower system	Gongguoqiao (GGQ)	900	Daily	3.2
	Xiaowan (XW)	4,200	Multiyear	149.1
	Manwan (MW)	1,670	Seasonal	9.2
	Dachaoshan (DCS)	1,350	Seasonal	9.4
	Nuozhadu (NZD)	5,850	Multiyear	237.0
	Jinghong (JH)	1,750	Seasonal	11.4
Middle Jinsha cascaded hydropower system	Liyuan (LY)	2,400	Daily	7.7
	Ahai (AH)	2,000	Daily	8.8
	Jinanqiao (JAQ)	2,400	Daily	9.1
	Longkaikou (LKK)	1,800	Daily	5.1
	Ludila (LDL)	2,160	Daily	17.2
	Guanyinyan (GYY)	3,000	Weekly	20.7

hydropower installed capacity in Yunnan and they are mainly source export to other provinces, power system peak shaving depends mainly on the hydropower plants of these two CHSs. As shown in Fig. 2, Chusui, Puqiao, Jinzhong and Yongfu HVDC transmission lines mainly deliver electricity of LCCHS and JSCHS to Guangdong and Guangxi. Thus, this paper mainly considers these two CHSs and corresponding HVDC lines coordination with wind and solar power to shave peaks for the Yunnan power grid (YNPG), Guangdong power grid (GDPG) and Guangxi power grid (GXPG). Basic information of these hydropower plants appears in Table 1.

III. MODEL

A. UNCERTAIN DESCRIPTION OF WIND AND SOLAR POWER

Wind and solar power are weather-sensitive sources in the short-term, making it difficult to forecast output accurately [41]. Since both wind and solar power have the well-known aggregation effect [42], [43]. This paper aggregates wind power plants in the same region as a single virtual wind power plant, and aggregates solar plants as a virtual solar power plant. With historical data, non-parametric kernel density estimation is adopted to estimate the short-term forecast

error distribution:

$$\hat{f}_t(x) = \frac{1}{n_t h_t} \sum_{i=1}^{n_t} K\left(\frac{x - x_{t,i}}{h_t}\right) \tag{1}$$

This paper uses Gaussian kernel function. h_t is decided by a rule-of-thumb estimator in this paper [44]. For wind and solar power, the samples are:

$$x_{t,i}^{W} = \frac{P_{t,i}^{W,a} - P_{t,i}^{W,f}}{P_{t,i}^{W,f}} \tag{2}$$

$$x_{t,i}^{S} = \frac{P_{t,i}^{S,a} - P_{t,i}^{S,f}}{P_{t,i}^{S,f}} \tag{3}$$

This can get a set of forecast error probability density functions (PDFs) for wind and solar power as:

$$\Gamma\left(\boldsymbol{f}^{W}\right) = \left\{\hat{f}_1^{W}(x_1), \hat{f}_2^{W}(x_2), \cdots, \hat{f}_T^{W}(x_T)\right\} \tag{4}$$

$$\Gamma\left(\boldsymbol{f}^{S}\right) = \left\{\hat{f}_1^{S}(x_1), \hat{f}_2^{S}(x_2), \cdots, \hat{f}_T^{S}(x_T)\right\} \tag{5}$$

As wind and solar power perform differently in each season. This paper uses historical data of each season to build sample sets and estimates short-term forecast error PDFs and cumulative density functions (CDFs) for wind and solar power of each season.

B. OBJECTIVE

Peak shaving operation reduces the load peak-valley difference and keeps the residual load as smooth as possible, so that inflexible power sources like coal-fired thermal power and nuclear power can have higher efficiency. According to our previous practical work, the power grid peak shaving model objective can be represented by minimizing the difference of maximum and minimum of residual load [31], [45], as follows:

$$F_g = \min\left\{\max_{1\le t\le T}\left(D_{g,t}\right)\right\} \tag{6}$$

For regional power sources serving multiple power grids, this objective is:

$$F = \sum_{g=1}^{G} \omega_g F_g = \sum_{g=1}^{G} \omega_g \cdot \min\left\{\max_{1\le t\le T}\left(D_{g,t}\right)\right\} \tag{7}$$

The residual load of power system g can be expressed as:

$$D_{g,t} = L_{g,t} - P_{g,t} \tag{8}$$

in which, $P_{g,t}$ can be expressed as following:

$$P_{g,t} = \begin{cases} \sum_{r\in\Omega_g} P_{r,t}, & g \text{ is client grid serving by HVDC} \\ P_t - \sum_{b=1,b\neq g}^{G} P_{b,t}, & g \textit{ is} \text{ host grid} \end{cases} \tag{9}$$

and P_t can be expressed as:

$$P_t = \sum_{m=1}^{M} P_{m,t}^{H} + P_t^{W,f} + P_t^{S,f} \tag{10}$$

The min-max objective function is not easy to solve directly. A single power grid objective function (6) can be recast to a linear equivalent form by introducing supplementary variables as:

$$F_g = \min\left\{A_g - B_g + \frac{1}{T}\sum_{t=1}^{T} D_{g,t}\right\} \tag{11}$$

in which A_g and B_g as the supplementary variables which represents the boundary of residual load of power grid g, can be expressed as:

$$\begin{cases} A_g = \max\limits_{1\le t\le T}\left\{D_{g,t}\right\} \\ B_g = \max\limits_{1\le t\le T}\left\{D_{g,t}\right\} \end{cases} \tag{12}$$

For multiple power grids, the objective function (7) can be recast to:

$$F = \min\left\{\sum_{g=1}^{G}\omega_g\left(A_g - B_g + \frac{1}{T}\sum_{t=1}^{T} D_{g,t}\right)\right\} \tag{13}$$

Then the objective is cast as linear form.

C. CONSTRAINTS

1) SYSTEM CONSTRAINTS

a: SYSTEM RESERVE REQUIREMENTS

$$\sum_{m=1}^{M}\left(P_{m,t}^{H,max} - P_{m,t}^{H}\right) \ge \sum_{g=1}^{G}\delta_g \times L_{g,t}; \quad \forall t \tag{14}$$

$$\sum_{m=1}^{M} P_{m,t}^{H} \ge \sum_{g=1}^{G}\delta_g \times L_{g,t}; \quad \forall t \tag{15}$$

These constraints represent positive and negative reserve capacity required by each power grid for hydropower.

b: TRANSMISSION LIMIT

$$\underline{P}_l^{L} \le P_{l,t}^{L} \le \bar{P}_l^{L}; \quad \forall t, \ \forall l \tag{16}$$

where $P_{l,t}^{L}$ is the transmission power of line l at period t. $\underline{P}_l^{L}$ and $\bar{P}_l^{L}$ are the lower and upper transmission capacity of line l. This constraint represents the capacity limitation of some key transmission lines.

2) OPERATION CONSTRAINTS OF HVDC

a: LOWER AND UPPER POWER LIMIT OF HVDC

$$\underline{P}_r \le P_{r,t} \le \overline{P}_r; \quad \forall r, \ \forall t \tag{17}$$

b: RAMPING CAPACITY OF THE HVDC LINE

$$\begin{cases} P_{r,t} - P_{r,t-1} = \Delta P^{+}_{r,t} + \Delta P^{-}_{r,t} \\ \Delta P^{+}_{r,t} \le b^{+}_{r,t} \Delta \bar{P}^{+}_{r} \\ \Delta P^{-}_{r,t} \ge b^{-}_{r,t} \Delta \bar{P}^{-}_{r} \\ b^{+}_{r,t} + b^{-}_{r,t} \le 1 \\ \Delta P^{+}_{r,t} > 0 \\ \Delta P^{-}_{r,t} < 0 \\ b^{+}_{r,t}, b^{-}_{r,t} \in \{0, 1\} \end{cases} ; \quad \forall r, \ \forall t \qquad (18)$$

where $b^{+}_{r,t}$ and $b^{-}_{r,t}$ are auxiliary binary variables to mark if the power is change positive or negative at period t. When change is positive, that means $P_{r,t} - P_{r,t-1} > 0$, with the constraints $b^{+}_{r,t} + b^{-}_{r,t} \le 1$, then $b^{+}_{r,t} = 1$, $b^{-}_{r,t} = 0$ and $\Delta P^{+}_{r,t} > 0$, $\Delta P^{-}_{r,t} = 0$; when change is negative, then $b^{+}_{r,t} = 0$, $b^{-}_{r,t} = 1$, and $\Delta P^{+}_{r,t} = 0$, $\Delta P^{-}_{r,t} < 0$; when there's no change, then $b^{+}_{r,t} = 0$, $b^{-}_{r,t} = 0$, and $\Delta P^{+}_{r,t} = 0$, $\Delta P^{-}_{r,t} = 0$.

c: STAIR-LIKE POWER CURVE CONSTRAINTS

HVDC power transmission curve should not fluctuate frequently and should remain stair-like to avoid misoperation of converter equipment. This constraint can be expressed as:

$$\begin{cases} \sum_{\tau=t}^{t+T^{M}_{r}-1} b^{+}_{r,t} \le u^{+}_{r,t} \cdot T^{M}_{r} \\ \sum_{\tau=t}^{t+T^{M}_{r}-1} b^{-}_{r,t} \le u^{-}_{r,t} \cdot T^{M}_{r} \\ u^{+}_{r,t} + u^{-}_{r,t} \le 1 \\ u^{+}_{r,t}, u^{-}_{r,t} \in \{0, 1\} \\ t \in [1, T - T^{M}_{r} + 1] \end{cases} ; \quad \forall r, \ \forall t \qquad (19)$$

where $u^{+}_{r,t}$ and $u^{-}_{r,t}$ are used to mark if the power is change positive or negative during periods $[t, t + T^{M}_{r} - 1]$. When $u^{+}_{r,t} = 1$, which means $u^{-}_{r,t} = 0$ and HVDC power increases during periods $[t, t + T^{M}_{r} - 1]$; When $u^{-}_{r,t} = 1$, then $u^{+}_{r,t} = 0$ and HVDC power decreases during periods $[t, t + T^{M}_{r} - 1]$; When $u^{-}_{r,t} = 0$ and $u^{+}_{r,t} = 0$, then HVDC power keeps unchanged.

d: MAXIMUM DAILY REGULATION TIMES OF HVDC LINES

HVDC lines are sensitive to faults and other abnormal conditions, frequently regulate HVDC power requires to convert HVDC converters many times and require host and client sides to regulate simultaneously, which may impact the grid stability. Therefore, the power grid dispatching department usually limits the maximum adjustment number in a reasonable range [46], [47]. This constraint can be expressed as:

$$\sum_{t=1}^{T} (b^{+}_{r,t} + b^{-}_{r,t}) \le C_r; \quad \forall r \qquad (20)$$

e: DAILY ELECTRICITY TRANSMISSION BOUNDS

$$\underline{E}_g \le \sum_{t=1}^{T} P_{g,t} \Delta t \le \overline{E}_g; \quad \forall g \qquad (21)$$

Generally, $\underline{E}_g$ and $\overline{E}_g$ are determined according to the trading results of the electricity market.

3) HYDROPOWER CONSTRAINTS

a: WATER BALANCE CONSTRAINTS

$$S_{m,t+1} = S_{m,t} + \left(Q^{in}_{m,t} + \sum_{j \in U_m} Q^{out}_{j,t-\tau_{j,m}} - Q^{out}_{m,t} \right) \times \Delta t; \quad \forall t, \ \forall m \qquad (22)$$

where $Q^{out}_{m,t} = Q^{tur}_{m,t} + Q^{s}_{m,t}$.

b: RESERVOIR STORAGE CONSTRAINTS

$$\underline{S}_{m,t} \le S_{m,t} \le \bar{S}_{m,t}; \quad \forall t, \ \forall m \qquad (23)$$

c: DISCHARGE LIMIT CONSTRAINTS OF EACH PLANT

$$\underline{Q}^{out}_{m,t} \le Q^{out}_{m,t} \le \bar{Q}^{out}_{m,t}; \quad \forall t, \forall m \qquad (24)$$

d: TURBINE DISCHARGE CONSTRAINTS OF EACH PLANT

$$\underline{Q}^{tur}_{m,t} \le Q^{tur}_{m,t} \le \bar{Q}^{tur}_{m,t}; \quad \forall t, \forall m \qquad (25)$$

e: INITIAL STORAGE AND EXPECTED FINAL STORAGE

$$S_{m,0} = S_{m,beg}; \quad \forall m \qquad (26)$$

$$S_{m,T} \ge S_{m,end}; \quad \forall m \qquad (27)$$

f: POWER OUTPUT RAMPING CONSTRAINTS

$$\left| P^{H}_{m,t} - P^{H}_{m,t-1} \right| \le \Delta \bar{P}^{H}_{m}; \quad \forall t, \ \forall m \qquad (28)$$

4) COMPENSATE CONSTRAINTS FOR OUTPUT DEVIATION OF WIND AND SOLAR POWER

a: POSITIVE COMPENSATE CONSTRAINT

$$\Pr \left\{ \begin{array}{l} \left(\sum_{m=1}^{M} P^{H,max}_{m,t} - \sum_{g=1}^{G} \delta_g \times L_{g,t} \right) \\ + P^{AW,a}_{t} + P^{AS,a}_{t} \ge P_t \end{array} \right\} \ge \alpha; \quad \forall t \qquad (29)$$

where $(\sum_{m=1}^{M} P^{H,max}_{m,t} - \sum_{g=1}^{G} \delta_g \times L_{g,t})$ is the maximum output deduct system reserve. This constraint means that hydropower can compensate for wind and solar power with a confidence level of α when the actual output of new renewables is less than the forecasted value. This constraint assures the hybrid hydro-wind-solar system provides enough power to avoid power shortages.

As mentioned in Eq. (2) and Eq. (3), $P^{W,a}_{t} = P^{W,f}_{t}(1+x^{W}_{t})$ and $P^{S,a}_{t} = P^{S,f}_{t}(1+x^{S}_{t})$, with the CDFs estimated with Eq. (1), the forecast error of wind and solar power can be expressed as:

$$\begin{cases} x^{W}_{t} = F^{W-1}_{t}(1-\alpha) \\ x^{S}_{t} = F^{S-1}_{t}(1-\alpha) \end{cases} \qquad (30)$$

Substitute this and Eq. (10) into constraint (29), it can be converted to the deterministic form:

$$\sum_{m=1}^{M} P_{m,t}^{H} \leq \left(\sum_{m=1}^{M} P_{m,t}^{H,max} - \sum_{g=1}^{G} \mu_g \times L_{g,t}\right) + P_t^{W,f} F_t^{W-1}(1-\alpha) + P_t^{S,f} F_t^{S-1}(1-\alpha) \quad (31)$$

b: NEGATIVE COMPENSATE CONSTRAINT

$$\Pr\left\{\begin{array}{l}\left(\sum_{m=1}^{M} P_{m,t}^{H,min} + \sum_{g=1}^{G} \mu_g \times L_{g,t}\right) + P_t^{AW,a} \\ + P_t^{AS,a} \leq P_t\end{array}\right\} \geq \beta \ \forall t \quad (32)$$

where $(\sum_{m=1}^{M} P_{m,t}^{H,min} + \sum_{g=1}^{G} \mu_g \times L_{g,t})$ is the minimum output considering system reserve. This constraint means that hydropower can reduce output to allocate for exceeded actual wind and solar power output with a confidence level of β to consume more new renewable generation.

Similarly, constraint (32) can be transformed to a deterministic form as:

$$\sum_{m=1}^{M} P_{m,t}^{H} \geq \left(\sum_{m=1}^{M} P_{m,t}^{H,min} + \sum_{g=1}^{G} \mu_g \times L_{g,t}\right) + P_t^{W,f} F_t^{W-1}(\beta) + P_t^{S,f} F_t^{S-1}(\beta) \quad (33)$$

These steps cast chance constraints into deterministic forms and transform the original problem into a deterministic optimization problem.

D. MILP BASED SOLUTION METHOD

As hydropower performance is usually a nonlinear function. The primal problem is a nonlinear optimization problem, which is difficult to solve directly. This paper uses linearization of hydropower performance function to recast it into MILP solvable problem.

Many studies assumed hydropower net head as constant for simplicity. However, for short-term operation, computation results may deviate from the accurate values greatly as net heads of some hydropower plants varies greatly in peak shaving. Assume that:

$$Q_{m,t}^{tur} = \begin{cases} Q_{m,t}^{out}, Q_{m,t}^{out} \leq \bar{Q}_{m,t}^{tur} \\ \bar{Q}_{m,t}^{tur}, Q_{m,t}^{out} > \bar{Q}_{m,t}^{tur} \end{cases} \quad (34)$$

which means that hydropower won't spill until the total discharge exceeds maximum turbine discharge or the output reach its maximum output; this is quite normal in hydropower operation. Then hydropower plant generation performance becomes:

$$\begin{cases} P_{m,t}^{H} = f_m^{gen}(H_{m,t}, Q_{m,t}^{tur}) \\ H_{m,t} = Z_{m,t}^{up} - Z_{m,t}^{down} - H_{m,t}^{loss} \\ Z_{m,t}^{up} = f_m^{ZV}((S_{m,t} + S_{m,t+1})/2) \\ Z_{m,t}^{down} = f_m^{ZQ}\left(Q_{m,t}^{out}\right) \\ H_{m,t}^{loss} = f_m^{loss}\left(Q_{m,t}^{tur}\right) \end{cases} \quad (35)$$

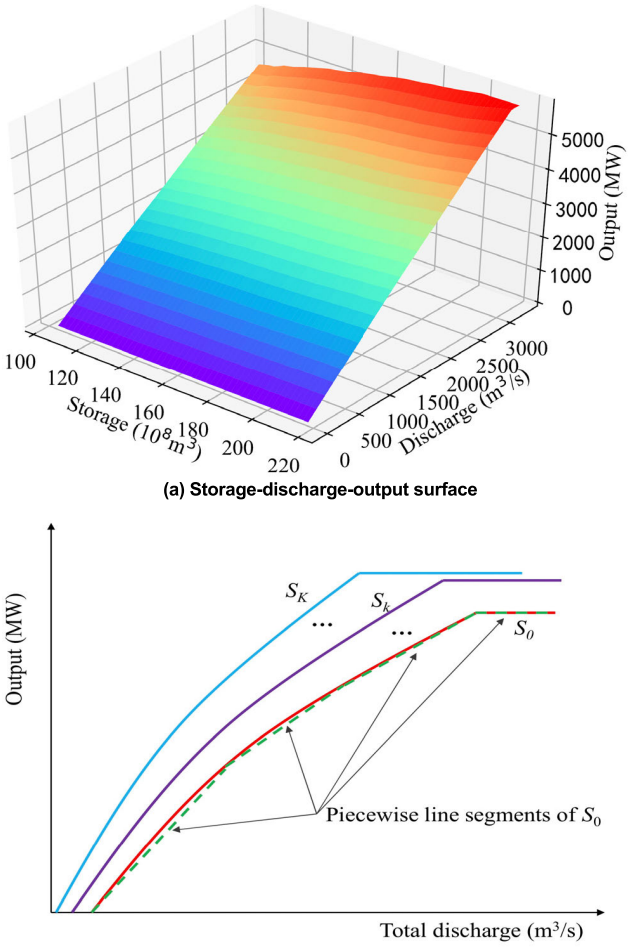

FIGURE 3. Sketch map of hydropower performance.

Thus, discrete storage and discharge, hydropower plant performance can be fitted as storage-discharge-output surface shown in Fig. 3(a) (it is a storage-discharge-output surface of a real hydropower plant in the study area). Furthermore, this performance surface can be dispersed and fitted as a set of discharge-output concave curves as shown in Fig. 3(b), each curve represents the discharge-output curve of a determine storage (or forebay water level). When the output of hydropower reaches the max output of current storage or the discharge reaches the max turbine discharge of current storage, then the output cannot increase with the increase of discharge any more. So, each curve in Fig. 3(b) has a horizontal tail (the effect of increasing discharge on the tail water level is ignored). Each is usually a non-linear concave curve. This paper uses piecewise linearization to fit concave discharge-output performance curve k as shown in Fig. 3(b) and express as [48], [49]:

$$\begin{cases} P_{m,k}^{H} = \sum_{l=1}^{L} a_{l,k} q_{l,k} \\ 0 \leq q_{l,k} \leq \bar{q}_{l,k} - \bar{q}_{l-1,k} \\ \bar{q}_{0,k} = 0 \end{cases} \quad (36)$$

For fixed-head hydropower plants that means only one discharge-output curve, the hydropower plant performance can be represented as Eq. (36). For head-sensitive hydropower plants with several discharge-output curves, their performance can be expressed as:

$$-P_{m,t}^{H,max}(1-v_{m,k}) \le P_m^H - P_{m,t}^H \le P_{m,t}^{H,max}(1-v_{m,k});\ \forall t, \forall k \tag{37}$$

in which:

$$\sum_{k=1}^{K_m} v_{m,k} = 1 \tag{38}$$

$$\sum_{j=1}^{k} v_{m,j} S_{m,j} \le S_m; \quad \forall t \tag{39}$$

$$\sum_{j=k}^{K_m} v_{m,j} S_{m,j+1} \ge S_m; \quad \forall t \tag{40}$$

$$v_{m,k} \in \{0, 1\}; \quad \forall k \tag{41}$$

Constraint (38) means only one interval can be chosen. Constraints (39)-(40) determine which interval is chosen. Constraints (37) compute the power production value. By this, the model is recast as a MILP solvable problem.

IV. RESULTS AND ANALYSIS

To test the effectiveness of the model, the following case studies applied the model in Yunnan's hybrid hydro-wind-solar power system quarter-hour day-ahead peak shaving scheduling. Since different power sources have different seasonal characteristics, especially as hydropower output varies considerably between dry and flood seasons. This paper uses typical daily data of these two seasons to test the model's effectiveness.

A. CASE STUDY 1: DRY SEASON PERFORMANCE

In this case, set confidence levels $\alpha = 0.9, \beta = 0.9$, allowable daily change time of HVDC lines $C_r = 10, T_r^M = 4, r \in [1, R]$. A typical load curve set of GDPG, GXPG and YNPG in the dry season is considered.

Table 2 shows the optimization results and the comparison with the original load and historical operation data as well. With the optimization of the proposed model, Table 2 indicates that the total peak valley difference decreases from 50,332 MW to 32,116 MW, a 36.2% reduction. For provincial grids, the peak-valley differences of GDPG, GXPG and YNPG reduce by 7,000 MW, 4,499 MW and 7,153 MW respectively, or 20.5%, 47.4% and 100% respectively. Besides, the load rates increase obviously, and the standard deviations decrease apparently for each power grid. Compare with the results of historical data, the proposed model performances much better in residual load peak-valley difference, load rate and standard deviation for each power grid since the conventional HVDC transmission line operation mode doesn't consider peak shaving requirement of the receiving power grids.

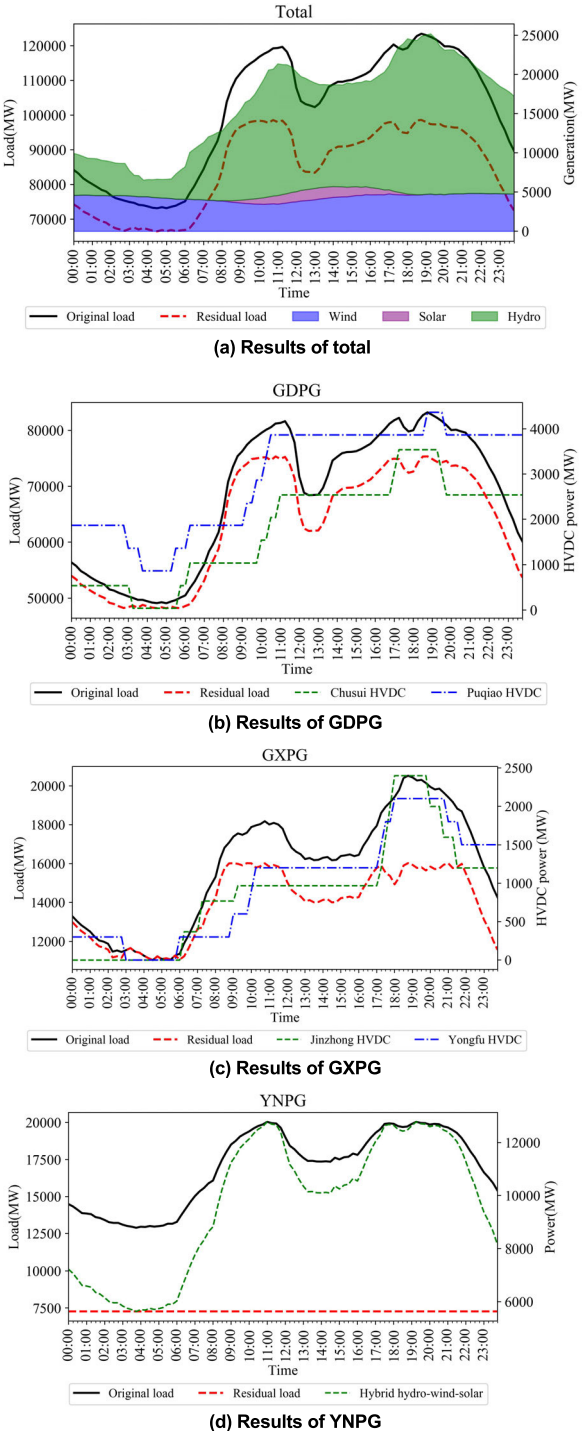

FIGURE 4. Optimal operation results of case 1.

Table. 3 shows the transmission power of each HVDC line. In addition, Fig.4 (a) shows quarter-hour output of each power source, original load and optimized residual load of the whole system. It shows that hydropower tries to cut peaks and compensate for anti-peak-regulation wind power. The original load and optimized load curves of each power grid and power of each HVDC transmission line appear in Fig. 4(b) – (d).

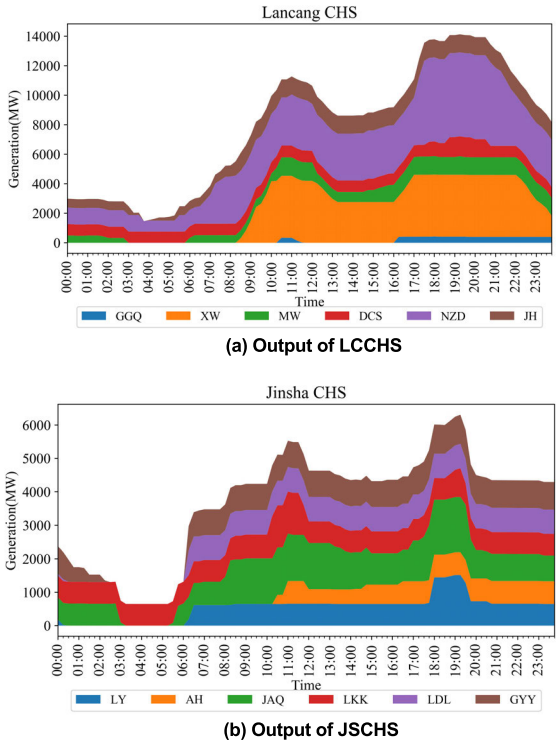

FIGURE 5. Power output of each plant of case 1.

Each line tries to shave peak loads as much as possible, increasing power load during peak periods and decreasing power during valley periods. With the regulation power of Chushui and Puqiao HVDC transmission lines, they help reduce the peak-valley difference of GDPG by 7,000 MW. Similarly, Jinzhong and Yongfu HVDC lines terminating at GXPG helps reduce the peak-valley difference greatly too. Fig. 4(c) shows the residual load of GXPG has small fluctuations during peak periods, mainly because HVDC lines have limited power regulation times, they can only shave the main peaks, and residual small fluctuations should be served by local power sources. Fig. 4(d) shows that YNPG has perfect straight-line residual load, meaning this model considers local peaking well. These results show that this hybrid hydro-wind-solar system can shave peaks effectively in the dry season.

Fig. 5 shows the quarter-hour output of each hydropower plant of these two CHSs. It clearly shows that each hydropower plant tries to participate in peak shaving, means that the proposed model can utilize the hydropower regulation capacity effectively. Furthermore, Since the hybrid hydro-wind-solar system has considered the forecast error, hydropower can offset the forecast error with the given confidence levels.

B. CASE STUDY 2: FLOOD SEASON PERFORMANCE

In this case, a typical flood season load curve is used to test the model. Table 4 indicates that, with the optimization of the

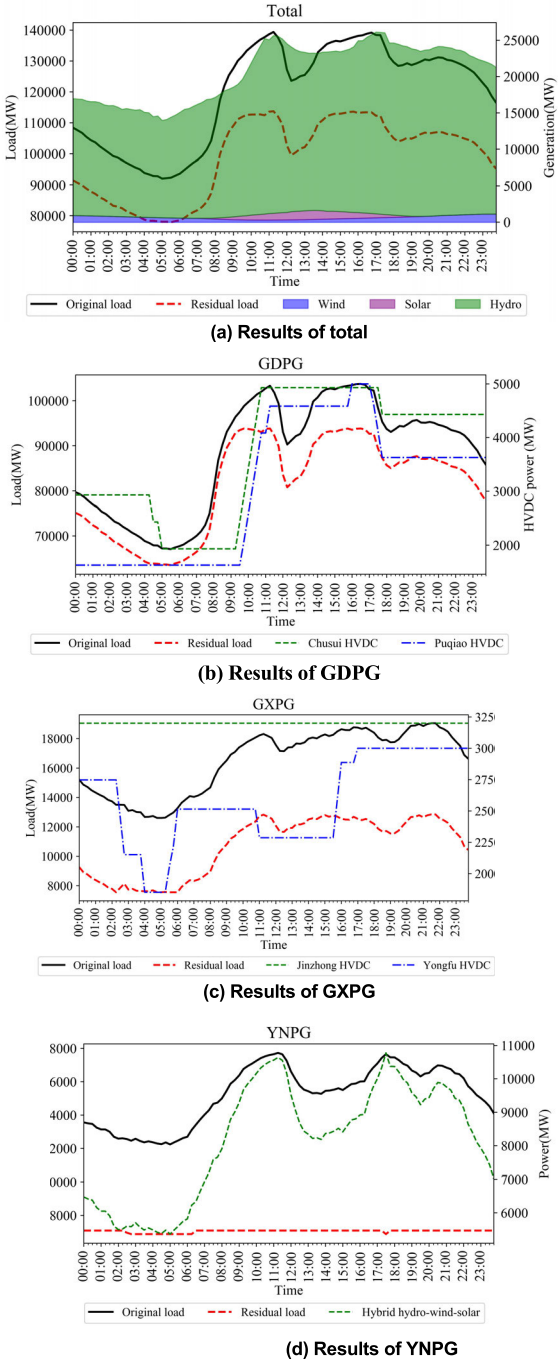

FIGURE 6. Optimal operation results of case 2.

proposed model, the total peak-valley difference decreased 24.3%, and this value of GDPG, GXPG and YNPG decreased 17.4%, 17.8% and 96.1%, respectively. Compare to the historical data, the results are much better for each power grid, verifies that this model is also effective during the flood season.

Fig. 6(a) indicates that hydropower tries to cut peak load, Fig. 6(b) - (d) indicate that HVDC transmission line try to

TABLE 2. Peak shaving results of multi-receiving power grids in case 1.

Item	Name	Peak load (MW)	Valley load (MW)	Peak-valley difference (MW)	Load rate (%)	Std. dev. (MW)
Total	Original load	123494	73,162	50,332	81.8	17,592
	Residual load (optimized)	98,622	66,506	32,116	85.9	12,107
	Residual load (historical)	102,963	63,356	39,607	82.8	13,353
GDPG	Original load	83,245	49,094	34,151	82.0	12,196
	Residual load (optimized)	75,342	48,191	27,151	84.3	10,368
	Residual load (historical)	76,145	47,494	28,651	83.4	9,936
GXPG	Original load	20,522	11,035	9,487	77.1	2,969
	Residual load (optimized)	16,022	11,034	4,988	87.1	1,795
	Residual load (historical)	18,072	9,485	8,587	77.2	2,652
YNPG	Original load	20,045	12,892	7,153	84.6	2,553
	Residual load (optimized)	7,258	7,258	0	100.0	0
	Residual load (historical)	20,521	14,074	6,447	83.8	1,892

Note: Peak-valley difference = Maximum – Minimum, Load rate = Average/ Maximum *100%

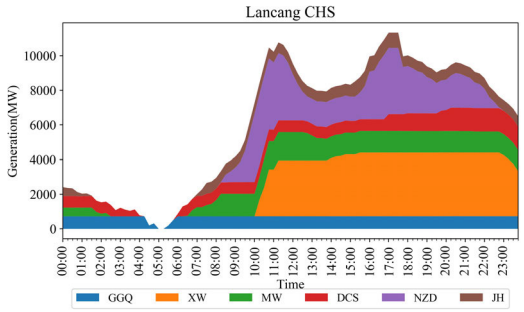

(a) Output of LCCHS

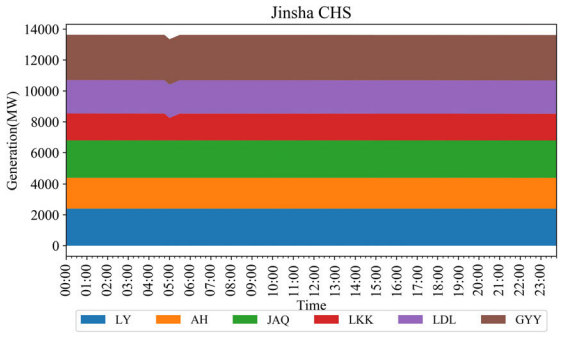

(b) Output of JSCHS

FIGURE 7. Power output of each plant of case 2.

shave the peak and each power grid get good result. However, there are some insights different from case 1: 1) As shown in Table 3 and 5, the average power of HVDC lines is much higher than in case 1, mainly because hydropower output is higher during the flood season and more hydropower generation needs to export to other regions via HVDC lines. 2) The peak-valley differences reduces by 6,373 MW, 1,149 MW and 5,277 MW in GDPG, GXPG and YNPG respectively, less than the corresponding values of case 1, especially GXPG.

TABLE 3. Power transmission indicates of each HVDC lines of case 1.

HVDC Line	Average (MW)	Max (MW)	Min (MW)	Load rate (%)	Std. dev. (MW)
Chushui	1,804	3,500	0	51	1,101
Puqiao	2,954	4,365	865	67.7	1,139
Jinzhong	889	2,399	0	37.1	703
Yongfu	973	2,101	0	46.3	690

Since stations in Jinsha River have small reservoirs (shown in Table 1), as shown in Fig. 7, with large inflow during the flood season, hydropower plants of JSCHS have less regulation ability, they can only reduce very limited output during valley periods and generate with full capacity during other periods. Peak shaving operation depends mainly on LCCHS, which have two huge reservoirs in Xiaowan and Nuozhadu hydropower plants. Since Jinzhong and Yongfu HVDC transmission lines mainly transmit generation of JSCHS, the average power of these two lines are much more than corresponding values of case 1. On the contrary, the average power of Puqiao and Chusui UHVDC lines which mainly transmit hydropower of LCCHS are a little higher than these values in case 1. 3) Wind power is much less than in case 1 as wind in Yunnan is weaker during the flood season and has lower power output, which is contrary to hydropower generation. The seasonal output characteristics of wind power and hydropower means that they have seasonal complementarity.

C. SENSITIVITY ANALYSIS OF DAILY REGULATION TIMES OF HVDC LINES

This subsection describes the sensitivity analysis of different allowable daily regulation times for HVDC lines.

TABLE 4. Peak shaving results of multi-receiving power grids in case 2.

Item	Name	Peak load (MW)	Valley load (MW)	Peak-valley difference (MW)	Load rate	Std. dev. (MW)
Total	Original load	139,396	92,053	47,343	86.0	16,264
	Residual load (optimized)	113,755	77,936	35,819	87.1	12,596
	Residual load (historical)	115,846	77,237	38,609	86.0	13,072
GDPG	Original load	103,772	67,065	36,707	85.0	12,553
	Residual load (optimized)	93,842	63,508	30,334	86.7	10,638
	Residual load (historical)	95,772	63,065	32,707	85.0	10,932
GXPG	Original load	19,047	12,606	6,442	86.5	2,191
	Residual load (optimized)	12,847	7,554	5,293	83.3	2,016
	Residual load (historical)	13,147	7,106	6,042	81.6	2,012
YNPG	Original load	17,725	12,236	5,489	85.8	1,777
	Residual load (optimized)	7,086	6,874	212	99.5	80
	Residual load (historical)	10,833	7,967	2,866	86.9	809

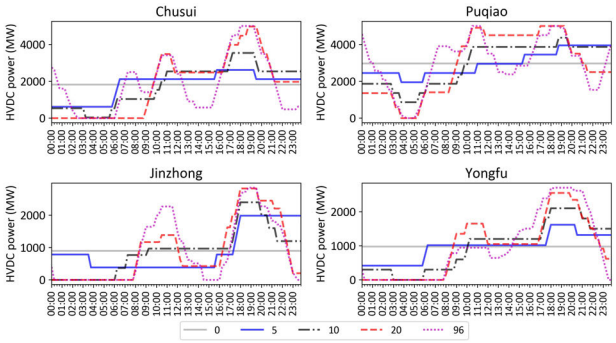

(a) Results of case 1

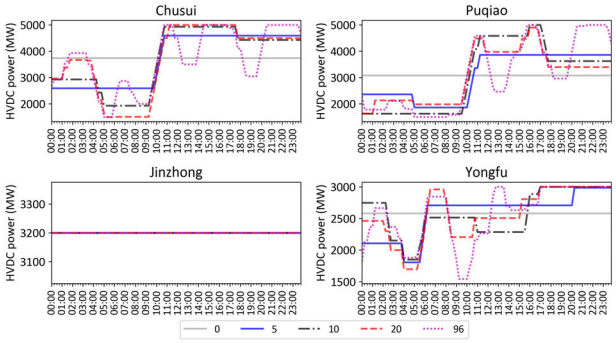

(b) Results of case 2

FIGURE 8. HVDC power of case 1 and case 2 under different allowable daily regulation times.

Table 6 lists results of case 1 and case 2 under different C_r, in which $C_r = 0$ means transmission power of HVDC lines are not allowed to change, $C_r = 96$ means no limitation of maximum change times (quarter-hour daily operation means 96 periods) and HVDC lines can change power each period.

TABLE 5. Power transmission indicates of each HVDC lines of case 2.

HVDC Lines	Average (MW)	Max (MW)	Min (MW)	Load rate (%)	Std. dev. (MW)
Chushui	3,733	4,931	1,931	75.7	1,158
Puqiao	3,068	5,000	1,627	61.4	1,284
Jinzhong	3,200	3,200	3,200	100	0
Yongfu	2,583	3,000	1,852	86.1	351

As shown in Table 6, as C_r just changes operation mode of HVDC lines, so residual load peak-valley difference of YNPG changes little, whereas the HVDC receiving power grids (GDPG and GXPG) change obviously with the increase of C_r. The peak valley difference and standard deviation of residual load decrease while load rates increase with the increase of C_r, it means more flexible HVDC power regulation is helpful for peak shaving. Fig. 8 shows power of HVDC lines of these two cases under different allowable daily regulation times. Both Fig. 8(a) and Fig. 8(b) indicate that HVDC power changes more frequently with additional allowable daily regulation times. However, these changes become less sensitive to the increasing of C_r. When C_r increase from 0 to 5, the peak-valley differences decrease significantly, and decrease a lot when C_r increase from 5 to 10. Nevertheless, when it further increases from 10 to 20, the residual load peak-valley differences decrease less, and when C_r increase from 20 to 96 (no limit), the residual load peak-valley differences decrease very little. Since adjusting HVDC power requires good communication between host and client ends and may increase HVDC failure risk, appropriate daily power regulation times helps power system safety and peak shaving operation.

TABLE 6. Results under different allowable daily regulation times of HVDC lines.

Max change Times (Cr)	Name	Case 1			Case 2		
		Peak-valley difference (MW)	Load rate	Std. dev. (MW)	Peak-valley difference (MW)	Load rate	Std. dev. (MW)
0	Total residual	43,615	81	15,074	42,534	84.8	14,641
	GDPG residual	34,151	81	12,196	36,707	83.9	12,553
	GXPG residual	9,487	75	2,969	6,442	80.7	2,191
	YNPG residual	0	100	0	0	100	0
5	Total residual	36,815	84	13,526	37,634	86.2	12,986
	GDPG residual	30,151	83	11,162	32,707	85.4	11,193
	GXPG residual	6,687	82	2,405	5,264	83.2	1,916
	YNPG residual	0	100	0	0	100	0
10	shown in Table. 2 and Table. 4						
20	Total residual	28,264	89	10,764	35,318	87.3	12,808
	GDPG residual	24,178	87	9,408	30,292	86.7	10,913
	GXPG residual	4,109	92	1,456	5,142	83.3	1,958
	YNPG residual	0	100	0	124	99.8	41
96	Total residual	28,061	89	11,692	35,030	87.2	12,958
	GDPG residual	24,151	87	10,386	29,707	86.8	11,015
	GXPG residual	3,933	93	1,447	5,322	83.4	2,042
	YNPG residual	0	100	0	0	100	0

V. CONCLUSION

HVDC transmission lines with long-distance and high-capacity power deliver capacity are widely used to allocate energy and balance energy supply and consumption, and essential for accommodating large-scale renewable energy resources. Coordinating renewable energies with traditional hydropower is favorable for power dispatching and renewable energy accommodation. This study presents a new multiple power grids peak shaving model considering coordinated operation of the hydro-wind-solar generation system that serves both the local power grid and several regional power grids via HVDC transmission lines. This model uses hydropower to compensate for wind and solar power forecast error and considers maximum daily power regulation times of HVDC lines to ensure power system safety. This model cast chance constraints and non-linear constraints into linear forms so that the problem is recast as a mixed-integer linear programming problem. Case studies show that: 1) The proposed model can reduce the peak-loads of multiple power grids effectively, which results in residual loads of inner province power grid smooth and slashes peak load of the receiving power grids dramatically. 2) Hydropower can compensate for wind and solar power forecast error effectively and keep the hybrid hydro-wind-solar system operating on schedule with the given confidence level. 3) Appropriate maximum daily power regulation times of HVDC benefits peak shaving of receiving power grids and reduces power system operation risk.

With the fast growing demand for electricity, renewable energies like wind and solar power will continue to grow quickly in China, and more HVDC transmission projects will be built to transmit large scale renewable energy to load centers. Hence, this study of coordinated operation of hydropower with wind and solar power considering HVDC transmission constraints is essential for optimal power system operation in China in the future. Meanwhile, hydro, wind and solar power are favorable energy sources globally, so the proposed model may offer suggestions to power dispatching departments generally. Since hydropower resources are limited, further research can consider the coordinated operation of renewable energies with other power sources that transmit via HVDC lines.

REFERENCES

[1] B. Liu, S. Liao, C. Cheng, F. Chen, and W. Li, "Hydropower curtailment in Yunnan Province, southwestern China: Constraint analysis and suggestions," *Renew. Energy*, vol. 121, pp. 700–711, Jun. 2018.

[2] S. Zhou, Y. Wang, Y. Zhou, L. E. Clarke, and J. A. Edmonds, "Roles of wind and solar energy in China's power sector: Implications of intermittency constraints," *Appl. Energy*, vol. 213, pp. 22–30, Mar. 2018.

[3] Y. Hu and H. Cheng, "Displacement efficiency of alternative energy and trans-provincial imported electricity in China," *Nature Commun.*, vol. 8, no. 1, p. 14590, Apr. 2017.

[4] *2018 Natioinal Electric Power Industry Statistics Express*, China Electr. Council, Beijing, China, 2019.

[5] *Renewable Capacity Statistics 2019*, Int. Renew. Energy Agency, Abu Dhabi, United Arab Emirates, 2019.

[6] X. Yang, Y. Song, G. Wang, and W. Wang, "A comprehensive review on the development of sustainable energy strategy and implementation in China," *IEEE Trans. Sustain. Energy*, vol. 1, no. 2, pp. 57–65, Jul. 2010.

[7] W. Chen, H. Li, and Z. Wu, "Western China energy development and west to east energy transfer: Application of the western China sustainable energy development model," *Energy Policy*, vol. 38, no. 11, pp. 7106–7120, Nov. 2010.
[8] Z. Ming, L. Honglin, M. Mingjuan, L. Na, X. Song, W. Liang, and P. Lilin, "Review on transaction status and relevant policies of southern route in China's West–East Power Transmission," *Renew. Energy*, vol. 60, pp. 454–461, Dec. 2013.
[9] X. Zhou, J. Yi, R. Song, X. Yang, Y. Li, and H. Tang, "An overview of power transmission systems in China," *Energy*, vol. 35, no. 11, pp. 4302–4312, Nov. 2010.
[10] J. Y. Zhao, F. M. Zhang, F. G. Liu, and Y. H. Liu, *A New Configuration of Current Source Converter Applied in HVDC*. Boca Raton, FL, USA: CRC Press, 2015, p. 297.
[11] A. Fuchs, M. Imhof, T. Demiray, and M. Morari, "Stabilization of large power systems using VSC–HVDC and model predictive control," *IEEE Trans. Power Del.*, vol. 29, no. 1, pp. 480–488, Feb. 2014.
[12] A. E. MacDonald, C. T. M. Clack, A. Alexander, A. Dunbar, J. Wilczak, and Y. Xie, "Future cost-competitive electricity systems and their impact on US CO_2 emissions," *Nature Climate Change*, vol. 6, no. 5, pp. 526–531, May 2016.
[13] C. Su, C. Cheng, P. Wang, and J. Shen, "Optimization model for the short-term operation of hydropower plants transmitting power to multiple power grids via HVDC transmission lines," *IEEE Access*, vol. 7, pp. 139236–139248, 2019.
[14] J. Shen, X. Zhang, J. Wang, R. Cao, S. Wang, and J. Zhang, "Optimal operation of interprovincial hydropower system including Xiluodu and local plants in multiple recipient regions," *Energies*, vol. 12, no. 1, p. 144, Jan. 2019.
[15] Z.-K. Feng, W.-J. Niu, and C.-T. Cheng, "China's large-scale hydropower system: Operation characteristics, modeling challenge and dimensionality reduction possibilities," *Renew. Energy*, vol. 136, pp. 805–818, Jun. 2019.
[16] K. Sun, K.-J. Li, J. Pan, Y. Liu, and Y. Liu, "An optimal combined operation scheme for pumped storage and hybrid wind-photovoltaic complementary power generation system," *Appl. Energy*, vol. 242, pp. 1155–1163, May 2019.
[17] W. Liu, F. Zhu, J. Chen, H. Wang, B. Xu, P. Song, P.-A. Zhong, X. Lei, C. Wang, M. Yan, J. Li, and M. Yang, "Multi-objective optimization scheduling of wind–photovoltaic–hydropower systems considering riverine ecosystem," *Energy Convers. Manage.*, vol. 196, pp. 32–43, Sep. 2019.
[18] B. Zhou, G. Geng, and Q. Jiang, "Hydro-thermal-wind coordination in day-ahead unit commitment," *IEEE Trans. Power Syst.*, vol. 31, no. 6, pp. 4626–4637, Nov. 2016.
[19] B. Xu, F. Zhu, P.-A. Zhong, J. Chen, W. Liu, Y. Ma, L. Guo, and X. Deng, "Identifying long-term effects of using hydropower to complement wind power uncertainty through stochastic programming," *Appl. Energy*, vol. 253, Nov. 2019, Art. no. 113535.
[20] H. Zhang, W. Hu, R. Yu, and M. Tang, "Coordinated optimal short-term operation of hydro-wind-solar integrated systems," *Energy Procedia*, vol. 158, pp. 6260–6265, Feb. 2019.
[21] A. Gupta, A. Kumar, and D. K. Khatod, "Optimized scheduling of hydropower with increase in solar and wind installations," *Energy*, vol. 183, pp. 716–732, Sep. 2019.
[22] J. Shen, C. Cheng, R. Cao, Q. Shen, X. Li, Y. Wu, and B. Zhou, "Generation scheduling of a hydrodominated provincial system considering forecast errors of wind and solar power," *J. Water Resour. Planning Manage.*, vol. 145, no. 10, Oct. 2019, Art. no. 04019043.
[23] X. Wang, J. Chang, X. Meng, and Y. Wang, "Short-term hydro-thermal-wind-photovoltaic complementary operation of interconnected power systems," *Appl. Energy*, vol. 229, pp. 945–962, Nov. 2018.
[24] L. Lei, W. Julong, L. Mingying, and C. Ming, "A correction method for HVDC transmission plan considering the correlation between sending end new energy generation and receiving end loads," *Energy Procedia*, vol. 145, pp. 193–198, Jul. 2018.
[25] Y. Zuo and X. Li, "Game theory applied in system of renewable power generation with HVDC out-sending facilitated by hundred megawatts battery energy storage station," in *Proc. IEEE Symp. Ser. Comput. Intell. (SSCI)*, Dec. 2016, pp. 1–5.
[26] M. Brenna, F. Foiadelli, M. Longo, and D. Zaninelli, "Improvement of wind energy production through HVDC systems," *Energies*, vol. 10, no. 2, p. 157, Jan. 2017.
[27] C. Su, C. Cheng, P. Wang, J. Shen, and X. Wu, "Optimization model for long-distance integrated transmission of wind farms and pumped-storage hydropower plants," *Appl. Energy*, vol. 242, pp. 285–293, May 2019.
[28] K. Xie, J. Dong, H.-M. Tai, B. Hu, and H. He, "Optimal planning of HVDC-based bundled wind–thermal generation and transmission system," *Energy Convers. Manage.*, vol. 115, pp. 71–79, May 2016.
[29] M. Xu, L. Wu, H. Liu, and X. Wang, "Multi-objective optimal scheduling strategy for wind power, PV and pumped storage plant in VSC-HVDC grid," *J. Eng.*, vol. 2019, no. 16, pp. 3017–3021, Mar. 2019.
[30] J. Shen, C. Cheng, X. Cheng, and J. R. Lund, "Coordinated operations of large-scale UHVDC hydropower and conventional hydro energies about regional power grid," *Energy*, vol. 95, pp. 433–446, Jan. 2016.
[31] Z.-K. Feng, W.-J. Niu, and C.-T. Cheng, "Optimal allocation of hydropower and hybrid electricity injected from inter-regional transmission lines among multiple receiving-end power grids in China," *Energy*, vol. 162, pp. 444–452, Nov. 2018.
[32] J.-J. Shen, Q.-Q. Shen, S. Wang, J.-Y. Lu, and Q.-X. Meng, "Generation scheduling of a hydrothermal system considering multiple provincial peak-shaving demands," *IEEE Access*, vol. 7, pp. 46225–46239, 2019.
[33] Z.-K. Feng, W.-J. Niu, C.-T. Cheng, and X.-Y. Wu, "Peak operation of hydropower system with parallel technique and progressive optimality algorithm," *Int. J. Electr. Power Energy Syst.*, vol. 94, pp. 267–275, Jan. 2018.
[34] X.-Y. Wu, C.-T. Cheng, J.-J. Shen, B. Luo, S.-L. Liao, and G. Li, "A multi-objective short term hydropower scheduling model for peak shaving," *Int. J. Electr. Power Energy Syst.*, vol. 68, pp. 278–293, Jun. 2015.
[35] Y. Wang, M. Zhao, J. Chang, X. Wang, and Y. Tian, "Study on the combined operation of a hydro-thermal-wind hybrid power system based on hydro-wind power compensating principles," *Energy Convers. Manage.*, vol. 194, pp. 94–111, Aug. 2019.
[36] G. Notton, D. Mistrushi, L. Stoyanov, and P. Berberi, "Operation of a photovoltaic-wind plant with a hydro pumping-storage for electricity peak-shaving in an island context," *Sol. Energy*, vol. 157, pp. 20–34, Nov. 2017.
[37] C.-T. Cheng, X. Cheng, J.-J. Shen, and X.-Y. Wu, "Short-term peak shaving operation for multiple power grids with pumped storage power plants," *Int. J. Electr. Power Energy Syst.*, vol. 67, pp. 570–581, May 2015.
[38] C. Baorui, "Study on the coordinated development of clean energy in Yunnan Province," (in Chinese), *Yunnan Water Power*, vol. 32, pp. 134–137, Mar. 2016.
[39] *China Southern Power Grid*. Accessed: Oct. 23, 2019. [Online]. Available: http://www.csg.cn
[40] *China Electric Power Yearbook (2011–2018)*, China Electr. Power Yearbook Board, China Electr. Power Press, Beijing, China, 2018.
[41] C. Sun, Z. Bie, M. Xie, and J. Jiang, "Assessing wind curtailment under different wind capacity considering the possibilistic uncertainty of wind resources," *Electr. Power Syst. Res.*, vol. 132, pp. 39–46, Mar. 2016.
[42] D. Lingfors and J. Widén, "Development and validation of a wide-area model of hourly aggregate solar power generation," *Energy*, vol. 102, pp. 559–566, May 2016.
[43] M. H. Albadi and E. F. El-Saadany, "Overview of wind power intermittency impacts on power systems," *Electric Power Syst. Res.*, vol. 80, no. 6, pp. 627–632, Jun. 2010.
[44] D. W. Scott, *Multivariate Density Estimation: Theory, Practice, and Visualization*, 1st ed. Hoboken, NJ, USA: Wiley, 1992.
[45] Z.-K. Feng, W.-J. Niu, W.-C. Wang, J.-Z. Zhou, and C.-T. Cheng, "A mixed integer linear programming model for unit commitment of thermal plants with peak shaving operation aspect in regional power grid lack of flexible hydropower energy," *Energy*, vol. 175, pp. 618–629, May 2019.
[46] F. Xu, M. Tu, X. Xie, L. Shi, and L. Yu, "A new operation model of HVDC tie-line for promoting renewable energy accommodation," in *Proc. IEEE Int. Conf. Energy Internet (ICEI)*, May 2019, pp. 290–297.
[47] J. Sun, R. Polytechnic Institute, M. Li, Z. Zhang, T. Xu, J. He, H. Wang, and G. Li, "Renewable energy transmission by HVDC across the continent: System challenges and opportunities," *CSEE J. Power Energy Syst.*, vol. 3, no. 4, pp. 353–364, Dec. 2017.
[48] D. W. Davis, *Columbia River Reservoir System Analysis: Phase II*. Davis, CA, USA: Hydrologic Engineering Center, 1993.
[49] M. S. Dogan, *Integrated Water Operations in California: Hydropower, Overdraft, and Climate Change*. Davis, CA, USA: Univ. of California, 2015.

BENXI LIU was born in Pingxiang, Jiangxi, China, in 1987. He received the B.S. and Ph.D. degrees in hydraulic and hydropower engineering from the Dalian University of Technology, Dalian, China, in 2009 and 2015, respectively.

Since 2015, he has been a Lecturer with the Dalian University of Technology. His current research interests include hydropower system operations, electricity market, and integrated management of renewable energy resources.

JAY R. LUND was born in USA, in 1957. He received the B.A. degree in international relations and regional planning from the University of Delaware, in 1979, and the M.A. degree in geography and the B.S. and Ph.D. degrees in civil engineering from the University of Washington, Seattle, WA, USA, in 1983 and 1986, respectively.

He was an Assistant Professor, from 1987 to 1991, an Associate Professor, from 1991 to 1996, and a Professor, from 1996 to 2017, with the University of California at Davis. Since 2017, he has been a Distinguished Professor. He is the author of four books and more than 150 journal articles. His research interests include reservoir operation, large-scale water–environmental system management, water supply planning and management, and water transfers and markets. His greatest focus is in combining engineering, economic, and operations, research ideas and methods for solving water, and environmental problems.

Dr. Lund was elected to the U.S. National Academy of Engineering, in 2018.

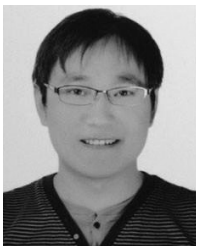

SHENGLI LIAO was born in Linxiang, Hunan, China, in 1980. He received the B.S. and Ph.D. degrees in hydraulic and hydropower engineering from the Dalian University of Technology, Dalian, China, in 2002 and 2009, respectively.

From 2009 to 2016, he has been a Lecturer with the Dalian University of Technology. Since 2017, he has been an Associate Professor. His current research interests include hydropower system operations and scheduling of clean energy for interconnected power grids.

XIAOYU JIN was born in Xinxiang, Henan, China, in 1995. He received the B.S. degree in hydraulic and hydropower engineering from Zhengzhou University, Zhengzhou, China, in 2018. He is currently pursuing the M.S. degree with the Institute of Hydropower and Hydroinformatics, Dalian University of Technology. His current research interests include optimization of hydropower systems and clean energy dispatching such as hydropower in the environment of electricity market.

LINGJUN LIU was born in Yuncheng, Shanxi, China, in 1996. She received the B.S. degree in hydraulic and hydropower engineering from Northwest A&F University, Shanxi, China, in 2018. She is currently pursuing the M.S. degree in water conservancy engineering with the Dalian University of Technology, Dalian, Liaoning, China.

Her current research interest includes hydropower system operations.

CHUNTIAN CHENG was born in Xiaogan, Hubei, China, in 1965. He received the Ph.D. degree in hydraulic engineering from the Dalian University of Technology, Dalian, China, in 1994.

Since 1999, he has been a Full Professor with the Dalian University of Technology. He is currently a Changjiang Distinguished Professor. He has authored more than 200 articles and more than 50 inventions. His research interests include optimal operation of large-scale hydropower systems, scheduling of clean energy for interconnected power grids, and electricity market.

Dr. Cheng was a recipient of the National Science Fund for Distinguished Young Scholars, in 2010.